Toward Astrophysical Turbulence in the Laboratory

G. G. Howes, D. J. Drake, K. D. Nielson, T. A. Carter, C. A. Kletzing, and F. Skiff

Toward Astrophysical Turbulence in the Laboratory

G. G. Howes,[1] D. J. Drake,[1,2] K. D. Nielson,[1] T. A. Carter,[3] C. A. Kletzing,[1] and F. Skiff[1]

[1]*Department of Physics and Astronomy, University of Iowa, Iowa City, Iowa 52242, USA.*
[2]*Department of Physics, Astronomy, and Geosciences,*
Valdosta State University, Valdosta, Georgia 31698, USA.
[3]*Department of Physics and Astronomy, University of California, Los Angeles, California 90095-1547, USA.*

Turbulence is a ubiquitous phenomenon in space and astrophysical plasmas, driving a cascade of energy from large to small scales and strongly influencing the plasma heating resulting from the dissipation of the turbulence. Modern theories of plasma turbulence are based on the fundamental concept that the turbulent cascade of energy is caused by the nonlinear interaction between counterpropagating Alfvén waves, yet this interaction has never been observationally or experimentally verified. We present here the first experimental measurement in a laboratory plasma of the nonlinear interaction between counterpropagating Alfvén waves, the fundamental building block of astrophysical plasma turbulence. This measurement establishes a firm basis for the application of theoretical ideas developed in idealized models to turbulence in realistic space and astrophysical plasma systems.

Introduction.—Turbulence profoundly affects many space and astrophysical plasma environments, playing a crucial role in the heating of the solar corona and acceleration of the solar wind [1], the dynamics of the interstellar medium [2–4], the regulation of star formation [5], the transport of heat in galaxy clusters [6], and the transport of mass and energy into the Earth's magnetosphere [7]. At the large length scales and low frequencies characteristic of the turbulence in these systems, the turbulent motions are governed by the physics of Alfvén waves [8], traveling disturbances of the plasma and magnetic field. Theories of Alfvénic turbulence based on idealized models, such as incompressible magnetohydrodynamics (MHD), suggest that the turbulent cascade of energy from large to small scales is driven by the nonlinear interaction between counterpropagating Alfvén waves [9–12]. However, the applicability of this key concept in the moderately to weakly collisional conditions relevant to astrophysical plasmas has not previously been observationally or experimentally demonstrated. Verification is important because the distinction between the two leading theories for strong MHD turbulence [11, 12] arises from the detailed nature of this nonlinear interaction. Furthermore, verification is required to establish the applicability of turbulence theories, utilizing simplified fluid models such as incompressible MHD, to the weakly collisional conditions of diffuse astrophysical plasmas.

Several reasons make it unlikely that the nonlinear interaction between counterpropagating Alfvén waves can ever be verified using observations of turbulence in astrophysical environments: the spatial resolution achievable in astrophysical observations is insufficient, *in situ* spacecraft measurements yield information at only a single or a few spatial points, and the broad spectrum of turbulent modes confounds attempts to identify the transfer of energy from two nonlinearly interacting Alfvén waves to a third wave. Only experimental measurements in the laboratory can achieve the controlled conditions and high spatial resolution necessary. The unique capabilities of the Large Plasma Device (LAPD) at UCLA [13], designed to study fundamental plasma physics processes, make possible the first laboratory measurement of the nonlinear wave-wave interaction underlying Alfvénic turbulence.

This Letter presents the first laboratory measurement of the nonlinear interaction between counterpropagating Alfvén waves, the fundamental building block of astrophysical plasma turbulence. The properties of the nonlinear daugther Alfvén wave are predicted from incompressible MHD theory. The experimental setup and procedure are outlined. Analysis of the experimental results demonstrate a successful measurement of the nonlinear interaction between counterpropagating Alfvén waves.

Theory.—Modern theories of anisotropic Alfvénic plasma turbulence are based on several key concepts derived from the equations of incompressible MHD. These equations can be expressed in the symmetric form [14],

$$\partial \mathbf{z}^{\pm}/\partial t \mp (\mathbf{v}_A \cdot \nabla)\mathbf{z}^{\pm} = -(\mathbf{z}^{\mp} \cdot \nabla)\mathbf{z}^{\pm} - \nabla p/\rho_0, \quad (1)$$

where the magnetic field is decomposed into $\mathbf{B} = \mathbf{B}_0 + \delta\mathbf{B}$, $\mathbf{v}_A = \mathbf{B}_0/\sqrt{\mu_0\rho_0}$ is the Alfvén velocity due to the equilibrium field $\mathbf{B}_0$, p is total pressure (thermal plus magnetic), ρ_0 is mass density, and $\mathbf{z}^{\pm} = \mathbf{v}_\perp \pm \delta\mathbf{B}_\perp/\sqrt{\mu_0\rho_0}$ are the Elsässer fields of the Alfvén waves which are incompressible, so that $\nabla \cdot \mathbf{z}^{\pm} = 0$. The Elsässer field $\mathbf{z}^+$ ($\mathbf{z}^-$) represents an Alfvén wave traveling down (up) the mean magnetic field. The second term on the left-hand side of (1) is the linear term representing the propagation of the Elsässer fields along the mean magnetic field at the Alfvén speed, the first term on the right-hand side is the nonlinear term representing the interaction between counterpropagating waves, and the second term on the right-hand side ensures incompressibility [11].

Consider the nonlinear interaction between two plane Alfvén waves with wavevectors $\mathbf{k}_1$ and $\mathbf{k}_2$, each with nonzero components both parallel and perpendicular to the

equilibrium magnetic field. The mathematical form of the nonlinear term in (1) requires two conditions for nonlinear interaction to occur: (a) both $\mathbf{z}^+ \neq 0$ and $\mathbf{z}^- \neq 0$, so the two waves must propagate in opposite directions along the magnetic field, implying $k_{\parallel 1}$ and $k_{\parallel 2}$ have opposite signs [9, 15]; and, (b) the polarizations of the perpendicular wave magnetic fields are not parallel, implying $\mathbf{k}_{\perp 1} \times \mathbf{k}_{\perp 2} \neq 0$. These properties dictate that the fundamental building block of plasma turbulence is the nonlinear interaction between perpendicularly polarized, counterpropagating Alfvén waves.

For sufficiently small amplitudes, the terms on the right-hand side of (1) are small compared to the linear propagation term, producing a state of *weak MHD turbulence* [10]. Note that the linear term in (1) has no counterpart in incompressible hydrodynamics, eliminating the possibility of weak turbulence, a fundamental distinction between incompressible hydrodynamic and incompressible MHD systems. In the weak MHD turbulence paradigm, two counterpropagating Alfvén waves interact nonlinearly to transfer energy to a third wave. This is the fundamental interaction underlying the cascade of energy to small scales in plasma turbulence. Solving for the nonlinear evolution using perturbation theory demonstrates that the nonlinear three-wave interaction, averaged over many wave periods, must satisfy the constraints

$$\mathbf{k}_1 + \mathbf{k}_2 = \mathbf{k}_3 \quad \text{and} \quad \omega_1 + \omega_2 = \omega_3, \qquad (2)$$

equivalent to the conservation of momentum and energy [10, 16, 17]. Given the dispersion relation for Alfvén waves, $\omega = |k_\parallel| v_A$, and the requirement for counterpropagating waves, the only nontrivial solution to these equations has either $k_{\parallel 1} = 0$ or $k_{\parallel 2} = 0$. [18]

The frequency constraint in (2) ceases to hold when the interaction spans only a fraction of a wave period. For such brief interactions, energy is transferred nonlinearly to a daughter mode at the instantaneous rate given by the nonlinear term in (1). In the laboratory, this can be accomplished by interacting a high-frequency Alfvén wave $\mathbf{k}_1$ with a counterpropagating Alfvén wave $\mathbf{k}_2$ of much lower frequency, such that its parallel wavelength is much longer than the length over which the waves interact. The physical effect of the low-frequency wave is to generate a shear in the equilibrium magnetic field, producing an effective $k_{\parallel 2} = 0$ component to the interaction. The predicted nonlinear product is an Alfvén wave $\mathbf{k}_3$ with the properties $k_{\parallel 3} = k_{\parallel 1}$ and $\mathbf{k}_{\perp 3} = \mathbf{k}_{\perp 1} + \mathbf{k}_{\perp 2}$.

Experiment.—The first experiment to verify this interaction in the laboratory was performed on the LAPD [13] using a background axial magnetic field of 800 G to confine a hydrogen plasma in a cylindrical column of 16.5 m length and 40 cm diameter. The plasma discharge exists for approximately 11 ms with a repetition rate of 1 Hz. The electron temperature, $T_e = 5.0$ eV, and density, $n = 10^{12}$ cm^{-3}, were determined using a swept Langmuir probe, with a microwave interferometer used
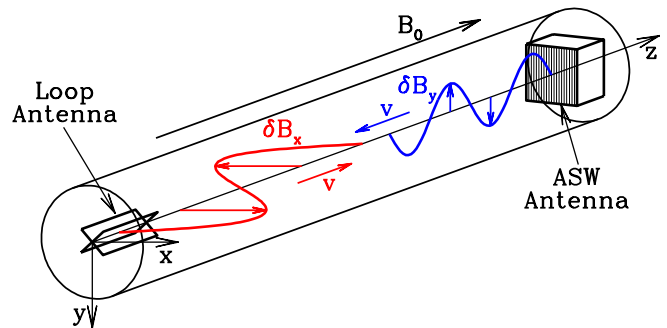

FIG. 1. Schematic of the Alfvén wave turbulence experiment on the LAPD. The Loop antenna generates a large-amplitude Alfvén wave polarized in the x-direction traveling up the mean magnetic field B_0 and the ASW antenna generates a smaller amplitude Alfvén wave polarized in the y-direction traveling down the mean magnetic field.

to calibrate density. The ion temperature, $T_i = 1.25$ eV, was estimated from previous interferometric measurements. For these parameters, the electron-ion collision frequency [19] is 3 kHz and the characteristic perpendicular scale is given by the ion sound Larmor radius $\rho_s = \sqrt{T_e/m_i}/\Omega_i = 0.29$ cm, where Ω_i is the ion cyclotron frequency.

The experimental setup is depicted in Fig. 1. At one end, the Arbitrary Spatial Waveform (ASW) antenna [20, 21] generates an Alfvén wave (blue) with frequency $f = 270$ kHz and a wave magnetic field polarized in the y-direction, δB_y, characterized by a precise perpendicular wavevector $\mathbf{k}_{\perp 1} \rho_s = 0.16\hat{\mathbf{x}}$. On the other end, a Loop antenna [22], constructed of two crossed current loops phased to produce a dominantly horizontal wave magnetic field δB_x, generates a large-amplitude Alfvén wave (red) with much lower frequency $f = 60$ kHz, characterized by a wavevector dominated by a y-component $k_{\perp 2y}\rho_s = 0.055$. The perpendicular wave magnetic fields, δB_x and δB_y, are measured using an Elsässer probe [23] between the antennas approximately 2 m from the Loop antenna and 9 m from the ASW antenna. The measurements are taken over a perpendicular plane of size 30 cm by 30 cm at a spacing of 0.75 cm, yielding a spatial grid of 41×41 measurement positions. At each position, 10 shots are averaged to improve the signal-to-noise ratio.

To generate a nonlinear interaction between the counterpropagating Loop and ASW Alfvén waves, first the Loop antenna is turned on and allowed to establish a steady wave pattern at $f = 60$ kHz. Next, the ASW antenna launches a perpendicularly polarized, counterpropagating wave. The spatial antenna waveform $\delta\mathbf{B}_\perp$, measured in single-antenna runs with identical timing, is presented in Fig. 2. Colormaps show the magnitude of (a) δB_x for the Loop antenna and (b) δB_y for the ASW antenna, and arrows show the vector direction of $\delta\mathbf{B}_\perp$. The ASW antenna produces a waveform of 30 mG peak-to-
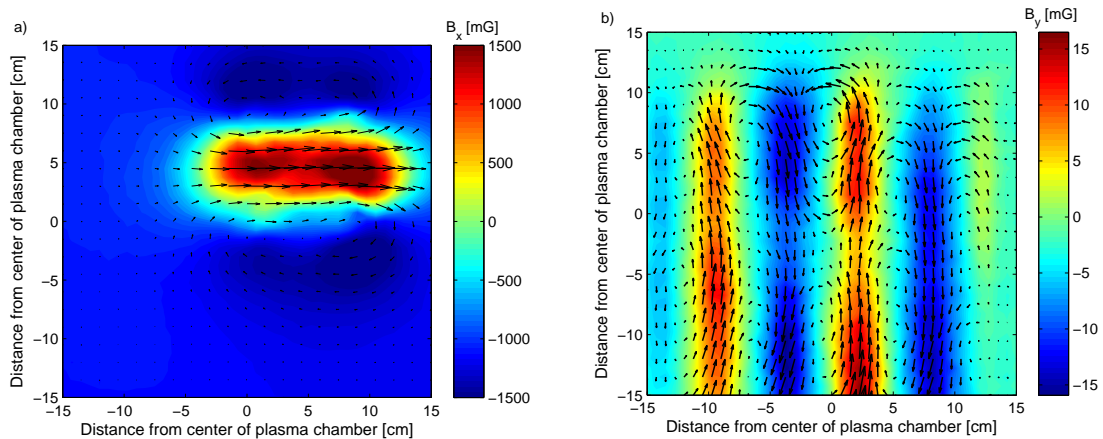
FIG. 2. Spatial magnetic-field waveforms from the (a) Loop antenna and (b) ASW antenna. The colormap indicates (a) δB_x for the Loop antenna and (b) δB_y for the ASW antenna in mG, and arrows indicate the vector direction of $\delta \mathbf{B}_\perp$.

peak amplitude with little δB_x component, whereas the Loop antenna produces a waveform of 3000 mG peak-to-peak amplitude that is dominated by the δB_x component.

The experimental results are presented in Fig. 3. We plot (b) the Fourier transform in the perpendicular plane, $\delta B_x(k_x, k_y, t)$, for the Loop antenna by itself and (c) $\delta B_y(k_x, k_y, t)$ for the ASW antenna by itself. Note that these are the spatial Fourier transforms of the antenna patterns in Fig. 2, and both antennas generate a pair of waves with $\pm \mathbf{k}_\perp$.

The analysis of the counterpropagating Alfvén wave run is designed to identify the nonlinear daughter Alfvén wave with two distinguishing properties: (a) $k_{\parallel 3} = k_{\parallel 1}$, which means the daughter wave will have the same frequency as the ASW wave, and (b) $\mathbf{k}_{\perp 3} = \mathbf{k}_{\perp 1} + \mathbf{k}_{\perp 2}$. First, to remove the linear contribution to δB_x caused by the large-amplitude Loop Alfvén wave, we subtract the signal of δB_x of the Loop-antenna-only run from the corresponding signal of the counterpropagating run to obtain $\delta B_x(x, y, t)$. Next, we Fourier transform in time the interval with both waves to obtain $\delta B_x(x, y, f)$. Since the signal of the daughter wave is expected to peak at the same frequency $f = 270$ kHz as the ASW wave, we band-pass filter the $\delta B_x(x, y, f)$ signal over the frequency range 170 kHz $\leq f \leq 370$ kHz, setting the Fourier coefficients to zero outside this range. The filtered frequency signal is then inverse Fourier transformed from frequency back to time. Finally, we Fourier transform in the perpendicular plane to obtain the spatial Fourier transform of the daughter wave, $\delta B_x(k_x, k_y, t)$.

The result of this procedure, shown in panel (d) of Fig. 3, is the key experimental result of this Letter. The observational signature of the nonlinear daughter Alfvén wave is clear, with the wave field δB_x dominated by four wavevectors, corresponding to all possible sums of perpendicular antenna wavevectors, $\mathbf{k}_{\perp 3} = +\mathbf{k}_{\perp 1} \pm \mathbf{k}_{\perp 2}$ and $\mathbf{k}_{\perp 3} = -\mathbf{k}_{\perp 1} \pm \mathbf{k}_{\perp 2}$, as shown schematically in panel (a)

of Fig. 3. The noise level of the subtracted signal in Fourier space is 1.2 mG cm^2, yielding a signal to noise ratio S/N $\gtrsim 10$, demonstrating that the measurement is physically meaningful. In addition, the amplitude of this nonlinear daughter Alfvén wave, which agrees to order of magnitude with theoretical expectations, peaks at the ASW wave frequency, $f_3 = 270$ kHz, as predicted. These results demonstrate that we have successfully measured the nonlinear interaction between counterpropagating Alfvén waves, the fundamental building block of astrophysical plasma turbulence.

This experimental finding verifies that the general properties of the nonlinear interaction between counterpropagating Alfvén waves, as derived theoretically in the idealized context of incompressible MHD, hold even under the weakly collisional conditions relevant to many space and astrophysical plasma environments. Although these conditions formally require a kinetic description of the turbulent dynamics, our results indicate that the key concepts derived from reduced fluid models describe the essential nature of the turbulent interactions. Future experiments will probe the turbulent dynamics at smaller scales, providing guidance for the extension of existing turbulence theories into the uncharted regime of kinetic turbulence at scales below the ion sound Larmor radius, where the effects of wave dispersion and kinetic wave-particle interactions influence the turbulent dynamics.
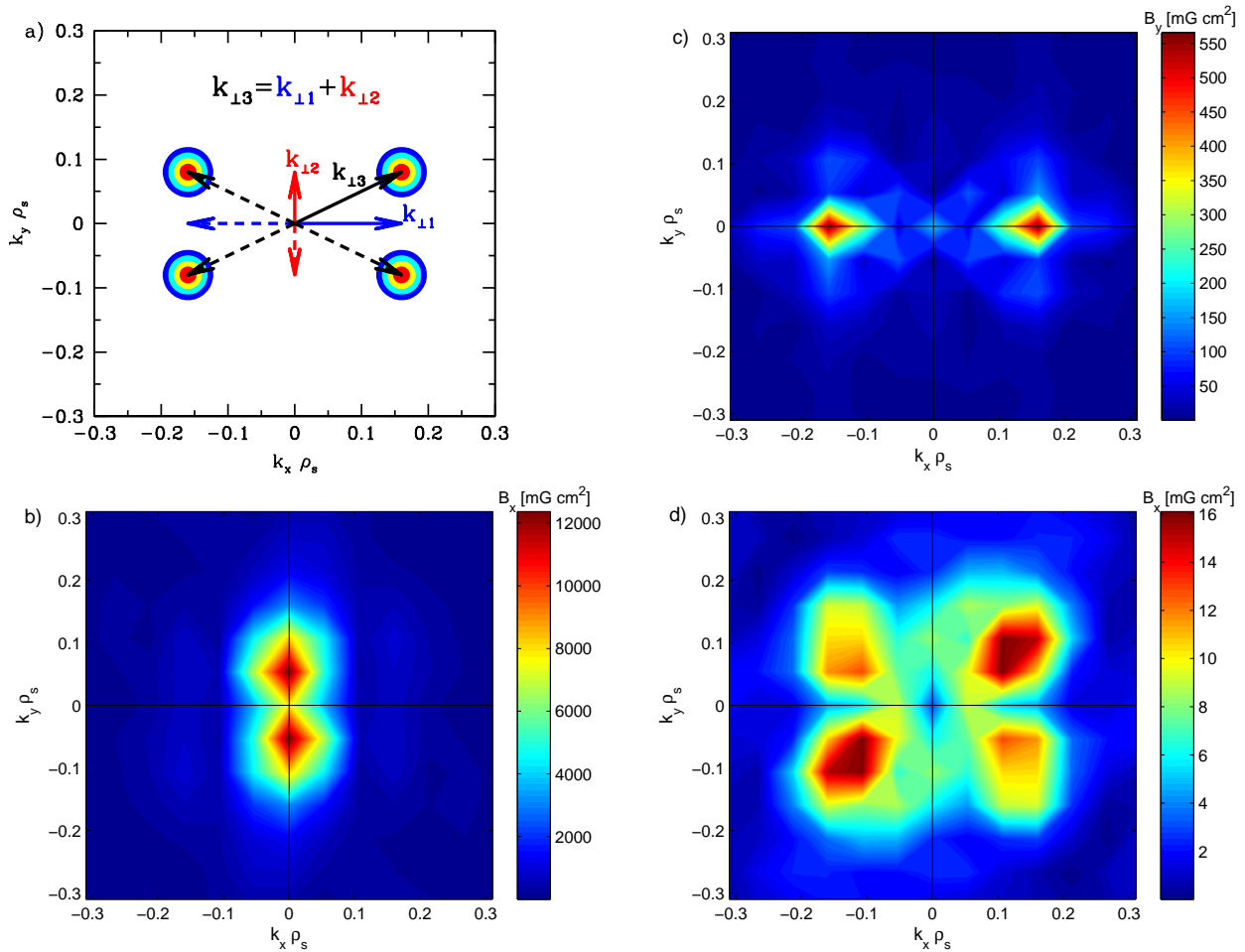
FIG. 3. (a) Diagram of $\mathbf{k}_\perp$ for the ASW antenna (blue) and Loop antenna (red). For the nonlinear daughter Alfvén wave, $\mathbf{k}_{\perp 3}$ (black) is the vector sum of the two antenna wave vectors, $\mathbf{k}_{\perp 3} = +\mathbf{k}_{\perp 1} \pm \mathbf{k}_{\perp 2}$ and $\mathbf{k}_{\perp 3} = -\mathbf{k}_{\perp 1} \pm \mathbf{k}_{\perp 2}$. Bullseyes indicate predicted power distribution of the nonlinear product. (b) Colormap of $\delta B_x(k_x, k_y)$ for the Loop antenna by itself. (c) Colormap (mG cm^2) of $\delta B_y(k_x, k_y)$ for the ASW antenna by itself. (d) Colormap of $\delta B_x(k_x, k_y)$ for the nonlinear daughter Alfvén wave.

[1] S. W. McIntosh, B. de Pontieu, M. Carlsson, V. Hansteen, P. Boerner, and M. Goossens, Nature **475**, 477 (2011).

[2] J. W. Armstrong, J. M. Cordes, and B. J. Rickett, Nature **291**, 561 (1981).

[3] J. W. Armstrong, B. J. Rickett, and S. R. Spangler, Astrophys. J. **443**, 209 (1995).

[4] B. M. Gaensler, M. Haverkorn, B. Burkhart, K. J. Newton-McGee, R. D. Ekers, A. Lazarian, N. M. McClure-Griffiths, T. Robishaw, J. M. Dickey, and A. J. Green, Nature **478**, 214 (2011).

[5] B. J. Rickett, Ann. Rev. Astron. Astrophys. **28**, 561 (1990).

[6] J. R. Peterson and A. C. Fabian, Phys. Rep. **427**, 1 (2006).

[7] D. Sundkvist, V. Krasnoselskikh, P. K. Shukla, A. Vaivads, M. André, S. Buchert, and H. Rème, Nature **436**, 825 (2005).

[8] H. Alfvén, Nature **150**, 405 (1942).

[9] R. H. Kraichnan, Phys. Fluids **8**, 1385 (1965).

[10] S. Sridhar and P. Goldreich, Astrophys. J. **432**, 612 (1994).

[11] P. Goldreich and S. Sridhar, Astrophys. J. **438**, 763 (1995).

[12] S. Boldyrev, Phys. Rev. Lett. **96**, 115002 (2006).

[13] W. Gekelman, H. Pfister, Z. Lucky, J. Bamber, D. Leneman, and J. Maggs, Review of Scientific Instruments **62**, 2875 (1991).

[14] W. M. Elsasser, Physical Review **79**, 183 (1950).

[15] R. S. Iroshnikov, Astron. Zh. **40**, 742 (1963), English Translation: Sov. Astron., 7 566 (1964).

[16] C. S. Ng and A. Bhattacharjee, Astrophys. J. **465**, 845 (1996).

[17] S. Galtier, S. V. Nazarenko, A. C. Newell, and A. Pouquet, J. Plasma Phys. **63**, 447 (2000).

[18] J. V. Shebalin, W. H. Matthaeus, and D. Montgomery, J. Plasma Phys. **29**, 525 (1983).

[19] S. I. Braginskii, Rev. Plasma Phys. **1**, 205 (1965).

[20] D. J. Thuecks, C. A. Kletzing, F. Skiff, S. R. Bounds, and S. Vincena, Phys. Plasmas **16**, 052110 (2009).

[21] C. A. Kletzing, D. J. Thuecks, F. Skiff, S. R. Bounds,

and S. Vincena, Phys. Rev. Lett. **104**, 095001 (2010).

[22] D. W. Auerbach, T. A. Carter, S. Vincena, and P. Popovich, Phys. Plasmas **18**, 055708 (2011).

[23] D. J. Drake, C. A. Kletzing, F. Skiff, G. G. Howes, and S. Vincena, Rev. Sci. Instr. **82**, 103505 (2011).